

A Carbon-13 and Deuterium NMR Investigation of Solid Platinum–Ethylene Complexes: Zeise's Salt and Pt(η^2 -C₂H₄)(PPh₃)₂

Guy M. Bernard, Roderick E. Wasylishen,* and Andrew D. Phillips

Department of Chemistry, Dalhousie University, Halifax, Nova Scotia, Canada B3H 4J3

Received: December 20, 1999; In Final Form: June 13, 2000

The carbon chemical shift (CS) tensors for two platinum–ethylene complexes, ethylene-¹³C₂-bis(triphenylphosphine)platinum(0) and potassium trichloro(ethylene-¹³C₂)platinate(II), have been characterized by the dipolar-chemical shift method and with 2D spin–echo NMR experiments. The carbon CS tensors of the ethylene ligand are significantly modified upon coordination with platinum, particularly for the Pt(0) complex, to which ethylene is strongly coordinated. The most shielded principal component, δ_{33} , perpendicular to the molecular plane in ethylene, is relatively unaffected by coordination; the changes to the CS tensors arise mainly from the increased shielding in the directions corresponding to δ_{11} and δ_{22} . Hence, the span of the chemical shift tensor decreases from 210 ppm for ethylene (Zilm, K. W.; Conlin, R. T.; Grant, D. M.; Michl, J. *J. Am. Chem. Soc.* **1980**, *102*, 6672) to 150 ppm for the Pt(II) complex, and to 48 and 55 ppm, respectively, for the two nonequivalent carbon nuclei of the Pt(0) complex. The orientations of the carbon CS tensor components relative to the ¹³C,¹³C dipolar vector are also determined from this analysis. Orientations of the carbon CS tensors in the molecular framework are proposed on the basis of a combination of the experimental results and ab initio calculations using the GIAO method. Deuterium NMR studies of the ethylene-²H₄ derivatives of the title compounds are characterized by long ²H T₁s and by quadrupolar coupling constants which are comparable in magnitude to that observed for rigid olefins, demonstrating that the ethylene ligand is not subject to significant motion. This conclusion is supported by ab initio calculations which indicate barriers to internal rotation for the ethylene ligand in excess of 80 kJ mol⁻¹ in both complexes.

Introduction

The preparation, by William Christopher Zeise in 1827, of potassium trichloro(ethylene)platinate(II), commonly known as Zeise's salt,¹ launched the field of organometallic chemistry. Despite being known for nearly two centuries, the physical and electronic properties of Zeise's salt and of its Pt(0) analogue, ethylenebis(triphenylphosphine)platinum(0), or Pt(C₂H₄)(PPh₃)₂, are not fully understood.² The objective of the present study is to gain a better understanding of the carbon chemical shift (CS) tensors in these complexes. In particular, we are interested in examining how the carbon CS tensors of the olefin are modified upon coordination with Pt(0) and Pt(II) centers. There have been numerous solution NMR studies of platinum–olefin complexes, but these yield only the isotropic shift corresponding to the average of the trace of the CS tensor; solid-state NMR affords the opportunity to determine the carbon CS tensor components. In addition, there have been conflicting reports about the dynamics of the ethylene ligand in Zeise's salt.² Understanding the internal dynamics of molecules, an important molecular property in itself, is particularly important here since a proper interpretation of the ¹³C NMR data requires knowledge of the motion of the nuclei under investigation. Hence, this study was undertaken to characterize the ethylenic³ carbon CS tensors for Pt(C₂H₄)(PPh₃)₂ and Zeise's salt and to investigate the dynamics of the ethylene ligands in these fundamental platinum–olefin complexes.

Here we present the results of a solid-state ¹³C NMR study of ¹³C₂-labeled samples of Pt(C₂H₄)(PPh₃)₂ and Zeise's salt. By

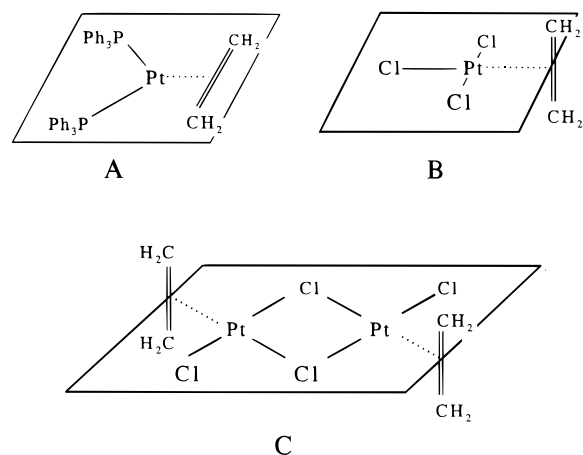
introducing double ¹³C-labeling in the ethylene ligand, it was possible to determine the magnitudes of the principal components of the carbon CS tensors and the orientations of the principal components relative to the ¹³C,¹³C dipolar vector (\mathbf{r}_{CC}).^{4,5} Although no further orientation information is available from the dipolar-chemical shift method,⁵ there is increasing evidence that CS tensor orientations may be reliably determined through ab initio calculations.⁶ Hence, orientations for the CS tensors in the molecular framework are proposed on the basis of ab initio calculations using the gauge-independent atomic orbitals (GIAO) method.⁷

Deuterium NMR is a well-established technique for probing molecular dynamics.⁸ By preparing ethylene-²H₄ derivatives of Pt(C₂H₄)(PPh₃)₂ and Zeise's salt, the dynamics of the ethylene ligand in these complexes can be investigated using ²H NMR. The dynamic properties derived from this study are corroborated by ab initio calculations.

Before presenting our results, it is useful to discuss the structures of these complexes and to review previous solid-state NMR studies of the title compounds.

Solid-State Molecular Structures. In Pt(C₂H₄)(PPh₃)₂ (Scheme 1A) the ethylene C,C bond is in the plane defined by the platinum and phosphorus atoms.⁹ The C,C bond length of the ethylene ligand, 1.434 ± 0.039 Å, is intermediate between that of uncoordinated ethylene, 1.338 ± 0.001 Å,¹⁰ and that of ethane, 1.5351 ± 0.0001 Å.¹¹ In contrast, X-ray diffraction studies of the anhydrous¹² and hydrate¹³ forms of Zeise's salt (Scheme 1B), as well as a neutron diffraction study of the latter,¹⁴ show that the ethylene ligand is oriented approximately perpendicular to the plane defined by the platinum and chlorine atoms. The C,C bond is only lengthened by 0.037 Å to 1.375

* To whom correspondence should be addressed. Present address: Department of Chemistry, University of Alberta, Edmonton, Alberta, Canada T6G 2G2. E-mail: Roderick.Wasylishen@ualberta.ca.

SCHEME 1: Structures of Pt(C₂H₄)(PPh₃)₂ (A), Zeise's Salt (B), and Zeise's Dimer (C)

Å¹³ compared to that of the free ligand. The ethylenic hydrogens are bent away from planarity,¹⁴ a situation which is thought to prevail for all substituents bound to olefinic³ carbons of such complexes.² The bonding of olefins to Pt(0) or Pt(II) is generally discussed in terms of a model proposed in the early 1950s by Dewar, Chatt, and Duncanson.¹⁵

Carbon-13 NMR Studies. The isotropic carbon chemical shift of olefinic carbons has been used extensively to investigate metal–olefin complexes in solution.¹⁶ For example, the isotropic magnetic shielding of the olefinic carbons of Pt(0) complexes increases by 60–80 ppm compared to that of the corresponding free ligand.¹⁷ However, few studies have reported the principal components of the olefinic carbon CS tensors in these complexes,¹⁸ and excluding Zeise's salt (vide infra), there have only been three studies of the olefinic carbon CS tensors of platinum–olefins. Wallraff reported the principal components of the olefinic carbon CS tensors for dichloro(1,5-cyclooctadiene)platinum(II).¹⁹ Gay and Young reported the principal components of the olefinic carbon CS tensors for several Pt–cyclooctadiene and Pt–norbornadiene complexes.²⁰ The olefinic carbon CS tensors for Pt(η^2 -*trans*-stilbene)(PPh₃)₂ were investigated by our laboratory.²¹ Apart from the latter study, only the magnitudes of the principal components of the carbon CS tensors were reported; their orientations in the molecular framework were not determined.

There have been numerous solution ¹³C NMR studies of Zeise's salt; the isotropic carbon chemical shifts determined from these studies range from 67.1 to 75.1 ppm,^{17a,22} compared to an isotropic carbon chemical shift of 126 ppm for ethylene.^{5c,23} There have also been some natural-abundance ¹³C NMR studies of solid magic-angle-spinning (MAS) samples of Zeise's salt. Huang and co-workers,²⁴ as well as Oldfield et al.,²⁵ reported the magnitudes of the principal components of the carbon CS tensors for Zeise's salt based on an analysis of the spinning sideband patterns of slow MAS samples. The analyses were based on the method of Herzfeld and Berger,²⁶ which does not provide any information about the orientation of the CS tensor. Ding and McDowell have carried out ¹³C NMR studies of slow MAS samples of Zeise's salt.²⁷ It appears that the authors have used the ^{35/37}Cl,¹³C dipolar interaction to obtain information about the anisotropy and orientation of the carbon CS tensors. Given that splittings due to ^{35/37}Cl,¹³C spin–spin coupling interactions are not resolved in the ¹³C NMR spectra of either spinning or stationary samples, it is unclear how reliable the orientation information is. There has been no ¹³C NMR study of stationary solid samples of Zeise's salt. In contrast to the

various ¹³C NMR studies of Zeise's salt, we are unaware of any previous report of the principal components of the carbon CS tensors for Pt(C₂H₄)(PPh₃)₂, although the isotropic carbon chemical shift was reported from ¹³C NMR of an MAS sample.²⁸

Dynamics of the Ethylene Ligand of Pt(C₂H₄)(PPh₃)₂ and Zeise's Salt. There have been numerous investigations of the internal ligand dynamics for metal–olefins in solution,²⁹ but the dynamics of ethylene in the solid state have rarely been investigated. Vierkötter and Barnes studied the dynamics of the ethylene ligand in solid Rh(acetylacetonato)(C₂H₄)₂ by ²H NMR and variable temperature ¹³C NMR, concluding that the ethylene undergoes both librational motion and 180° flips.³⁰ In their ¹³C NMR investigation of solid osmium–ethylene complexes, Lewis and co-workers concluded that the ethylene undergoes rotation about the axis perpendicular to the C,C bond, and that the barrier to internal rotation is comparable to values measured in solution.³¹

The dynamics of the ethylene ligand in solid samples of Zeise's salt and Zeise's dimer (Scheme 1C) have been studied by ¹H NMR. Through a second moment analysis³² of the ¹H NMR spectra of Zeise's dimer, Reeves concluded that the ethylene ligand undergoes a rocking motion about the axis perpendicular to the C,C bond.³³ In a later ¹H NMR study of Zeise's salt, Maričić et al.³⁴ concluded that, besides the rocking motion, the ethylene ligand also undergoes large-amplitude oscillations about the axis parallel to the C,C bond.

There appears to be uncertainty in the literature about the interpretation of these experimental results. For example, it has recently been stated that the ethylene ligand of Zeise's salt rotates rapidly in the solid state.²⁷ To clarify this point, and to properly interpret our ¹³C NMR data, we have undertaken a ²H NMR study of the internal dynamics of the ethylene ligands in Pt(C₂²H₄)(PPh₃)₂ and Zeise's salt-²H₄.

Experimental Section

Sample Preparation. Samples were prepared on the basis of procedures reported in the literature: that of Blake and Roundhill³⁵ for Pt(C₂H₄)(PPh₃)₂ and that of Chock et al.³⁶ for Zeise's salt. In all cases, the ethylene, either natural-abundance carbon, ¹³C₂-labeled (Isotec, 99% ¹³C) or ²H₄-labeled (Isotec, 99% ²H), was placed under a pressure of 2 atm in a reaction flask for at least 48 h prior to isolation of the product, rather than bubbling the ethylene through the reaction solution as recommended in refs 35 and 36. The samples were characterized by their melting points and by solution and solid-state NMR, as well as by electro-spray mass spectrometry in the case of Zeise's salt. To ensure consistent Zeise's salt samples, which hydrate slowly, these were dehydrated by placing them under dynamic vacuum (10⁻³ Torr) for 16 to 20 h.³⁶ Anhydrous samples were packed in sealed 4 mm NMR rotors under a dry nitrogen atmosphere.

NMR. Solid-state ¹³C NMR spectra were obtained on Chemagnetics CMX Infinity 200 ($B_0 = 4.7$ T, $\nu_0(^{13}\text{C}) = 50.3$ MHz) and Bruker AMX-400 ($B_0 = 9.4$ T, $\nu_0(^{13}\text{C}) = 100.6$ MHz) NMR spectrometers. Cross polarization under the Hartmann–Hahn match condition,³⁷ with contact times of 0.5 to 1 ms, high-power proton decoupling with ¹H 90° pulses of 3.5 to 4.5 μ s and recycle times of 60–300 s were used to acquire all ¹³C NMR spectra. All peak positions were referenced to TMS (l , 300 K) by setting the high-frequency isotropic peak of an external adamantane sample to 38.56 ppm.³⁸ Carbon-13 NMR spectra of the ¹³C₂-labeled sample of Pt(C₂H₄)(PPh₃)₂ were complicated by the contribution from the natural-abundance ¹³C nuclei of the six phenyl rings. This was removed by acquiring

a spectrum of the unlabeled sample under identical conditions as for the labeled sample and subtracting the FID of the former from the latter. Spectra were processed with line broadening functions of 0–10 Hz (MAS) or 200–400 Hz (stationary). Spectra of stationary powder samples were calculated using a computer program developed in this laboratory which incorporates the POWDER algorithm of Alderman et al.³⁹ The principal components of the carbon CS tensors are reported relative to TMS such that $\delta_{11} \geq \delta_{22} \geq \delta_{33}$, the latter being the most shielded component. The line shapes of the stationary powder spectra are described by the span, $\Omega = \delta_{11} - \delta_{33}$, and the skew, $\kappa = 3(\delta_{22} - \delta_{iso})/\Omega$, where δ_{iso} is the isotropic chemical shift.⁴⁰

Carbon-13 2D spin–echo NMR spectra were acquired on a Bruker AMX 400 spectrometer using a standard spin–echo pulse sequence,⁴¹ with experimental parameters similar to those used for the 1D experiments. The data size was 1024×128 after zero filling in both dimensions. The final spectra are displayed in the magnitude mode following the application of window functions in both dimensions. The *F1* projection was simulated using the program Spinecho, written in this laboratory. Uncertainties in all parameters are assigned by comparison of the calculated and experimental spectra.

NMR spectra of ¹³C₂-labeled samples were analyzed with the dipolar-chemical shift method. A detailed discussion of the method has been given elsewhere;^{4,5} we present here the important experimental aspects of the technique. The NMR spectrum of a dipolar-coupled spin pair is defined by up to 13 parameters: besides the dipolar coupling, $R(^{13}\text{C}, ^{13}\text{C})$, between the two nuclei, both CS tensors have three principal components (or equivalently, δ_{iso} , Ω , and κ) and three Euler angles defining their orientations.⁴² The indirect coupling, $^1J(^{13}\text{C}, ^{13}\text{C})$, is not resolved in ¹³C NMR spectra of stationary samples. Comparison of NMR spectra acquired at different applied magnetic fields differentiates spectral features arising from anisotropic chemical shielding and dipolar interactions, since the latter is independent of the applied magnetic field strength. Parameters may also be obtained from other experiments. If not complicated by other ¹³C nuclei, the NMR spectrum of a stationary sample containing a dilute spin will yield the principal components of the CS tensor. The spectrum of a slow MAS sample will yield δ_{iso} and provide insight into the values of Ω and κ . For example, spectra with small spans have a negligible spinning sideband pattern. Two-dimensional spin–echo experiments provide reliable values of $R(^{13}\text{C}, ^{13}\text{C})$.⁴³ Finally, information about CS tensor orientations is sometimes available from the local molecular symmetry,^{4,5} since the orientations of the CS tensors must be related by the same symmetry element relating the dipolar-coupled spin pair.

Deuterium NMR spectra of stationary powder samples were acquired at 300 K on the Bruker AMX-400 spectrometer, operating at a ²H NMR frequency of 61.4 MHz, using a quadrupolar echo pulse sequence.⁴⁴ Recycle delays of up to 90 min were required to obtain spectra with an acceptable signal-to-noise ratio. The ²H NMR line shapes for both samples have reflection symmetry about their centers; that for Pt(C₂H₄)(PPh₃)₂ was symmetrized, yielding a 2^{1/2} enhancement in the signal-to-noise ratio.⁴⁵ Deuterium NMR spectra, simulated using a program written in this laboratory, are described in terms of the ²H quadrupolar coupling constant, C_Q , and the asymmetry in the deuterium electric field gradient (EFG) tensor, η .

Ab Initio Calculations. The carbon CS tensors were calculated at the Hartree–Fock (HF) level of theory using the GIAO method⁷ with the Gaussian 98 suite of programs⁴⁶ mounted on an IBM RISC/6000 computer. Locally dense basis

sets⁴⁷ were used: cc-pVQZ for the ethylenic carbons, the LANL2DZ⁴⁸ effective core potential (ECP) for platinum, and 3-21G for the remaining atoms. The experimental geometries of Pt(C₂H₄)(PPh₃)₂⁹ and of the anion of Zeise's salt^{12,14} were used for all calculations. To keep the computational time of the shielding calculations within reasonable limits, the phenyl groups of Pt(C₂H₄)(PPh₃)₂ were replaced with methyl groups. The positions of the ethylenic hydrogen atoms of Pt(C₂H₄)(PPh₃)₂ were calculated at the HF/6-31G* level; those of Zeise's salt are from a neutron diffraction study of the hydrate form.¹⁴ For comparison, calculations were also performed on ethylene using the cc-pVQZ and 3-21G basis sets on carbon and hydrogen, respectively. The geometry of ethylene is that determined by Duncan.¹⁰ All carbon chemical shielding values were converted to chemical shifts by taking the absolute shielding of the TMS carbons to be 188.1 ppm⁴⁹ (i.e., $\delta(\text{calcd}) = 188.1 - \sigma(\text{calcd})$).

The barrier to internal rotation of the ethylene ligand in Zeise's salt was calculated by optimizing the structure of the anion at the second-order Møller–Plesset (MP2) level of theory⁵⁰ using the LANL2DZ ECP for platinum and the 6-31G* basis set for the remaining atoms. All structural parameters were optimized except the angle formed by the C,C bond with the plane defined by the platinum and three chlorine atoms, which was fixed at 15° increments between 0 and 90°. Similar calculations on Pt(C₂H₄)(PPh₃)₂ were impractical because of its size but single-point HF calculations at the 6-31G* level were performed, with the ethylene oriented in and at 90° to the plane defined by the platinum and phosphorus atoms.

Results and Discussion

Carbon-13 NMR Spectra of MAS and Stationary Samples.

The carbon CS tensors of Pt(C₂H₄)(PPh₃)₂ and Zeise's salt are discussed separately, followed by a discussion contrasting these tensors with those of ethylene.

Carbon-13 NMR Spectra of Pt(C₂H₄)(PPh₃)₂. Carbon-13 NMR spectra of MAS samples of Pt(C₂H₄)(PPh₃)₂ are shown in Figure 1. The lower trace, a spectrum of the unlabeled sample, illustrates the large contribution from the phenyl ¹³C nuclei in natural abundance. Although of relatively low intensity, the contributions from the ethylenic carbon nuclei are apparent at approximately 39 ppm, in agreement with previous solid-state²⁸ and solution^{17a,51} NMR studies. The expansion of this region shows that there are two peaks, a consequence of the crystallographic nonequivalence of the ethylenic carbon atoms.⁹ Spinning sidebands, indicated by asterisks in Figure 1, are barely distinguishable at an MAS frequency (ν_{rot}) of 3725 Hz, demonstrating that the spans of the ethylenic carbon nuclei are not large. The spectrum of the ¹³C₂-labeled sample is shown in the upper trace of Figure 1; the expansion of the ethylenic region indicates the presence of two peaks. These peaks are invariant to ν_{rot} or B_0 , confirming that they arise from chemically nonequivalent ethylenic carbon nuclei.⁵² There is no evidence of indirect spin–spin coupling to ¹⁹⁵Pt (natural abundance, 33.8%) or ³¹P; not surprising since the reported values of $^1J(^{13}\text{C}, ^{195}\text{Pt})$ and $^2J(^{13}\text{C}, ^{31}\text{P})$ measured in solution, 194 and 24 Hz, respectively,^{17a} are significantly smaller than the half-height line widths of the spectra of MAS samples, approximately 250 Hz.

Figure 2 illustrates the 2D ¹³C spin–echo NMR spectrum of Pt(C₂H₄)(PPh₃)₂. The *F1* projection, shown at the right of this figure, was calculated with the same parameters as for the calculation of the 1D NMR spectra, discussed below. The calculated spectrum is very sensitive to R_{eff} :

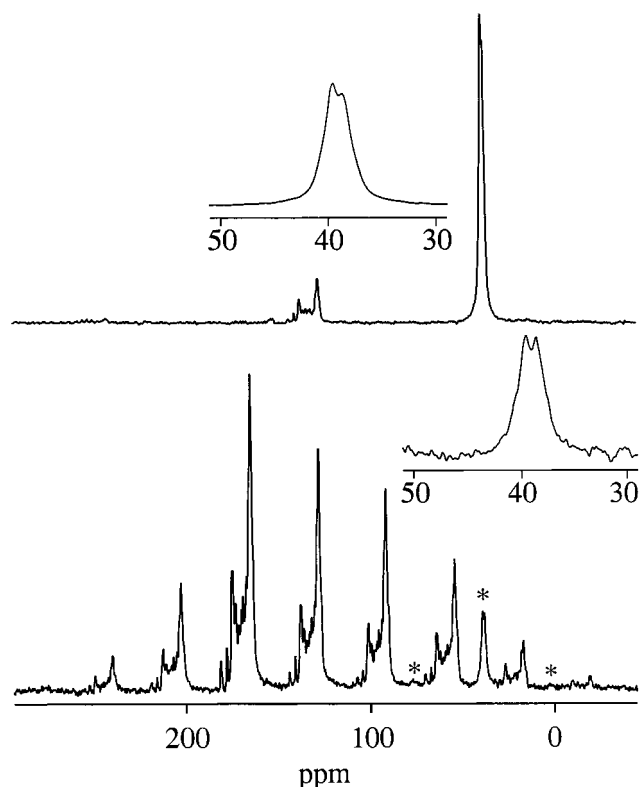


Figure 1. Carbon-13 NMR spectra of MAS samples of Pt(C₂H₄)-(PPh₃)₂. The lower trace is a spectrum of the unlabeled sample, acquired at 9.4 T with $\nu_{\text{rot}} = 3725$ Hz; 476 transients were acquired. The isotropic peak and first-order spinning sidebands of the ethylenic carbon nuclei are indicated with asterisks. The upper trace is that of the ¹³C₂-labeled sample acquired at 9.4 T with $\nu_{\text{rot}} = 11500$ Hz; 24 transients were added. The insets are expansions of the isotropic peaks for the ethylenic carbon nuclei.

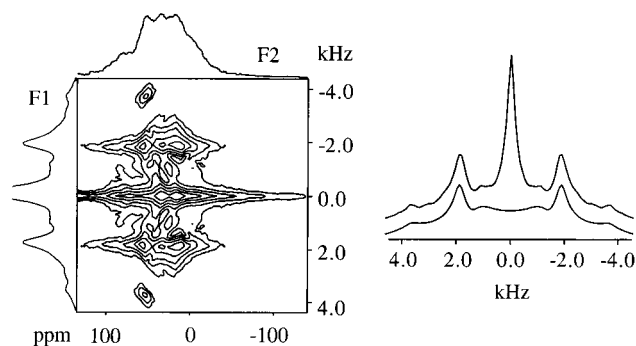


Figure 2. Two-dimensional ¹³C spin-echo NMR spectrum of Pt-(¹³C₂H₄)(PPh₃)₂ acquired at 9.4 T; 56 transients were added for each of 64 t_1 increments. At right, the experimental (top) and calculated (bottom) F1 projections are shown. The central peak is an experimental artifact.

$$R_{\text{eff}} = R_{\text{DD}} - \frac{\Delta J}{3} \quad (1)$$

where R_{DD} is the direct dipolar coupling constant (eq 2) and ΔJ is the anisotropy in the indirect (J) coupling tensor.

$$R_{\text{DD}} = \left(\frac{\mu_0}{4\pi} \right) \left(\frac{\hbar}{2\pi} \right) \gamma_C^2 \langle r_{\text{CC}}^{-3} \rangle \quad (2)$$

The term in angular brackets in eq 2 is the motionally averaged inverse cube of the internuclear separation. Although ΔJ for Pt(C₂H₄)(PPh₃)₂ is not known, it is approximately 11 Hz for ethylene.^{53,54} Hence $\Delta J/3$ is thought to be negligible⁵⁴ and

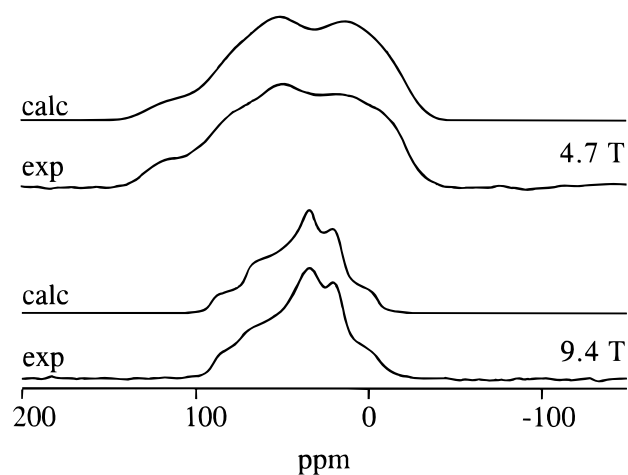


Figure 3. Calculated and experimental ¹³C NMR spectra of a stationary sample of Pt(¹³C₂H₄)(PPh₃)₂. The contribution of the natural-abundance aromatic ¹³C to the spectra have been removed by subtraction. 276 and 174 transients were added for spectra acquired at 4.7 and 9.4 T, respectively.

TABLE 1: Experimental and Calculated Carbon Chemical Shift Tensors^a for Ethylene, Pt(C₂H₄)(PPh₃)₂, and Zeise's Salt

	δ_{11}	δ_{22}	δ_{33}	δ_{iso}	Ω	κ	θ_{11}	θ_{22}	θ_{33}	α^b
Ethylene										
expt ^c	234	120	24	126	210	-0.09	90.0	0.0	90.0	0.0
calcd ^d	267	104	11	127	256	-0.27	90.0	0.0	90.0	0.0
Pt(C ₂ H ₄)(PPh ₃) ₂										
expt ^e	65	44	10	39.7	55	0.23	42	52	75	0
expt ^e	61	42	13	38.7	48	0.21	36	56	80	0
calcd ^d	48	22	-3	22.3	51	-0.02	81	15	78	0
calcd ^d	47	19	-3	21.0	50	-0.12	86	18	73	2
Zeise's Salt (anhydrous)										
expt ^e	150	79	0	76.0	150	0.06	84	14	103	0.0
calcd ^d	159	78	-3	78.0	162	0.00	89	4	94	0.0
calcd ^d	153	80	-3	76.7	156	0.06	90	3	94	0.0
Zeise's Salt (hydrate)										
calcd ^d	145	69	-6	69.3	151	-0.01	90	4	94	0.0
calcd ^d	158	77	-5	76.7	163	0.01	89	5	94	0.0

^a Chemical shifts are relative to TMS. ^b The torsion angle between the δ_{33} components. ^c From ref 5c; uncertainties are ± 2.5 ppm. ^d Calculated at the HF level using locally dense basis sets (see text) which included the cc-pVQZ basis set on the ethylenic carbon atoms. The nonequivalent carbon CS tensors calculated for the complexes are reported. ^e This work. The δ_{ii} are in ppm, with uncertainties of ± 5 ppm, except ± 0.5 ppm for δ_{iso} . The θ_{ii} and α are reported in degrees, with an uncertainty of $\pm 10^\circ$.

$R_{\text{DD}} \approx R_{\text{eff}}$, allowing an estimate of r_{CC} (eq 2). The experimental value of R_{eff} , 2475 ± 100 Hz, corresponds to a value of 1.453 ± 0.020 Å. This value is within experimental error of that determined from X-ray crystallography, 1.434 ± 0.039 Å.⁹ It is important to recognize that angular fluctuations of the dipolar vector arising from motion of the molecule or ligand also lead to averaging (a reduction) in R_{eff} .^{5c} The close agreement of r_{CC} values from the NMR and X-ray data suggests that motional averaging of the dipolar interaction is unimportant, a conclusion that is supported by the ²H NMR data (vide infra).

The simulated and experimental spectra of a stationary sample of Pt(C₂H₄)(PPh₃)₂ are shown in Figure 3; the parameters derived from the simulation are summarized in Table 1. The small chemical shift difference between the two ethylenic carbons results in a complex powder pattern, since most crystallites are oriented such that the two carbon nuclei comprise an AB spin system.⁵⁵

To discuss the orientations of the CS tensor components, it is useful to introduce the angle θ_{ii} which defines the angle formed by the tensor component δ_{ii} with \mathbf{r}_{CC} . The relative orientation of the two CS tensors may be described by the Euler angle α , which is equivalent to the torsion angle between the two δ_{33} components. The simulated spectra are sensitive to this parameter—values are summarized in Table 1. Because a simulated spectrum of a stationary sample is invariant to simultaneous rotation of the two CS tensors about \mathbf{r}_{CC} , the orientation of the CS tensor in the molecular framework cannot be unambiguously determined by the dipolar-chemical-shift method.^{5,21,56} For this, we turn to the results of ab initio calculations,⁶ discussed below.

Molecules with mirror symmetry planes which include the nuclei of interest have one CS tensor component perpendicular to this plane while the remaining two components lie in the plane. For $\text{Pt}(\text{C}_2\text{H}_4)(\text{PPh}_3)_2$, none of the principal components of the carbon CS tensors are oriented perpendicular to the plane defined by the platinum and ethylenic carbon atoms. This is attributed to the fact that $\text{Pt}(\text{C}_2\text{H}_4)(\text{PPh}_3)_2$ does not have a true mirror plane in the solid state.⁹ Since carbon shielding is sensitive to small differences in the local environment (vide infra) and the magnitudes of the principal components are comparable, small deviations from planarity can lead to significant changes to θ_{ii} .

Calculated Carbon CS Tensors for $\text{Pt}(\text{C}_2\text{H}_4)(\text{PPh}_3)_2$. The calculated ethylenic carbon CS tensor parameters for $\text{Pt}(\text{C}_2\text{H}_4)(\text{PPh}_3)_2$ are summarized in Table 1; those for ethylene are included for comparison. References to calculated values in the ensuing discussion are those obtained for the model compound, $\text{Pt}(\text{C}_2\text{H}_4)(\text{PMe}_3)_2$. Agreement between experimental and calculated carbon CS tensors is good although the magnitudes of the calculated principal components are usually shielded compared to the experimental values. The most striking feature of the experimental data is the large change in the span, $\Omega = 48$ and 55 ppm for $\text{Pt}(\text{C}_2\text{H}_4)(\text{PPh}_3)_2$, compared to that of ethylene, $\Omega = 210$ ppm,²³ and at the same time the insensitivity of δ_{33} to coordination. These features are qualitatively reproduced by the ab initio shielding calculations.

The calculated values of θ_{ii} are reported in Table 1. Calculated θ_{33} values are within error of the experimental values, but the calculated θ_{11} and θ_{22} are significantly different from the corresponding experimental values. Accurately calculating orientations for CS tensors with principal components which have similar magnitudes is particularly challenging. As well, it is important to recognize that the calculations are carried out on an isolated molecule while experimentally the molecule is subject to a variety of intermolecular interactions. Nevertheless, an accurately calculated θ_{33} combined with the results of an earlier study on a similar molecule²¹ allows us to propose an orientation for the carbon CS tensors in the molecular framework.

As discussed above, the absence of a component perpendicular to the Pt,C,C plane is not surprising. One is tempted to assume that the δ_{33} components are in this general direction, since θ_{33} is close to 90°; however, results of ab initio calculations on $\text{Pt}(\text{C}_2\text{H}_4)(\text{PMe}_3)_2$ suggest that this component is actually in the Pt,C,C plane, oriented such that it is approximately perpendicular to the plane defined by the methylene group. This is similar to the orientation of the δ_{33} components of the olefinic carbon CS tensor of a related compound, $\text{Pt}(\eta^2\text{-trans-stilbene})(\text{PPh}_3)_2$ ²¹ and is consistent with the observation that the direction of greatest shielding for olefins is always perpendicular to the molecular plane.^{23,57} Thus, based on the combined experimental—

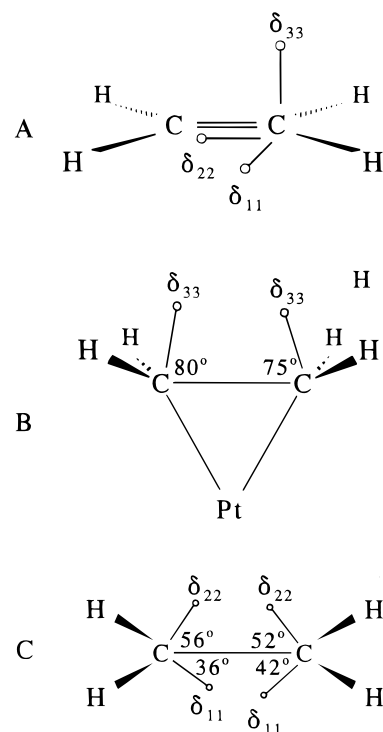


Figure 4. Orientation of the carbon CS tensors of ethylene (A).²³ In (B), the δ_{33} components of $\text{Pt}(\text{C}_2\text{H}_4)(\text{PPh}_3)_2$ are shown with the molecule oriented such that the platinum and ethylenic carbon atoms are in the plane of the page, together with δ_{33} . The remaining components are shown in (C), with the Pt,C,C plane perpendicular to the page. The numbers indicate the angle between the tensor components and \mathbf{r}_{CC} . Note that in (C) both δ_{11} and δ_{22} are not exactly in the plane of the page.

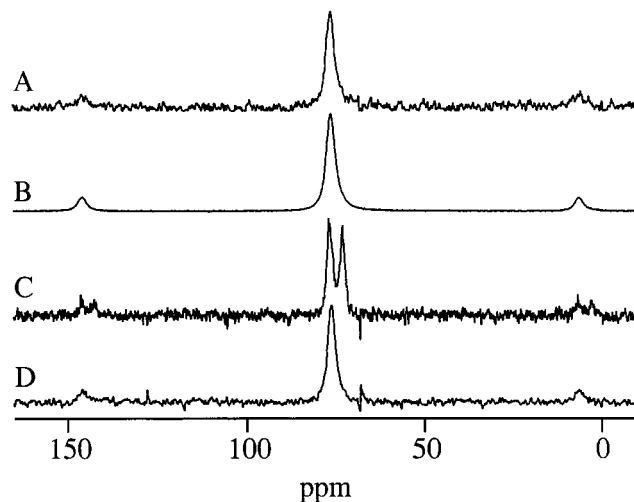


Figure 5. Carbon-13 NMR spectra of MAS samples of Zeise's salt: that of the natural-abundance carbon sample prepared in our lab (A), the $^{13}\text{C}_2$ -labeled sample (B), and of a commercial sample before (C) and after (D) dehydration. Spectra were acquired at 9.4 T with $\nu_{\text{rot}} = 7$ kHz; 104 (A), 64 (B), and 72 transients for both (C) and (D) were added.

theoretical results, the orientation of δ_{33} is assigned as shown in Figure 4B. The orientations of δ_{11} and δ_{22} follow from that of δ_{33} and the experimental values of θ_{11} and θ_{22} , as shown in Figure 4C. For comparison, the orientation of the carbon CS tensor for ethylene is shown in Figure 4A.

Carbon-13 NMR Spectra of Zeise's Salt. The ^{13}C NMR spectra of MAS samples of Zeise's salt are shown in Figure 5. In Figure 5A, the spectrum of a natural-abundance carbon

sample prepared in our laboratory is shown. The spectrum is very similar to that of the $^{13}\text{C}_2$ -labeled sample (Figure 5B) except that the line widths of the latter are spinning-frequency dependent. This arises from incomplete averaging of the $^{13}\text{C},^{13}\text{C}$ homonuclear dipolar coupling^{5c,52} and is often observed in samples containing a spin pair with crystallographically equivalent but magnetically nonequivalent sites.⁵² The half-height line widths of the isotropic peak of the unlabeled MAS sample is approximately 250 Hz. The fact that these peaks are broader than expected (for example, they are as broad as those observed for the nonequivalent sites of the spectra of MAS samples of $\text{Pt}(\text{C}_2\text{H}_4)(\text{PPh}_3)_2$) suggests that there is a contribution to the observed line shapes from the dipolar interaction with the chlorine atoms, which is not completely averaged by MAS.⁵⁸ For the $^{13}\text{C}_2$ -labeled samples, $\nu_{1/2} \approx 700$ Hz at $B_0 = 9.4$ T and $\nu_{\text{rot}} = 3$ kHz; with $\nu_{\text{rot}} = 12$ kHz, the line width is comparable to that observed for the unlabeled sample. The line widths observed for NMR spectra of MAS samples acquired at 4.7 T are comparable to those observed at twice the spinning frequency at 9.4 T, as expected.^{52b} Considering the observed line widths for these samples, it is not surprising that $^1J(^{13}\text{C},^{195}\text{Pt})$, approximately 195 Hz in solution NMR studies,^{17a,22} is not resolved in solid-state NMR spectra.

There are two striking differences between our spectra of the MAS samples (Figure 5 A and B) and those reported by Huang et al.²⁴ The latter authors observed two isotropic peaks in an unlabeled sample, attributed to nonequivalent carbon sites, and the values of δ_{iso} for these two peaks (63 and 61 ppm) are 13 and 15 ppm to low frequency of our single peak, $\delta_{\text{iso}} = 76$ ppm. Zeise's salt is known to crystallize in a hydrate form, space group $P2_1/c$,^{13,14} and in an anhydrous form, space group $Pmab$.¹² Suspecting that the two peaks observed by Huang et al. are separate peaks from the two crystal forms, we obtained a sample of Zeise's salt from the same supplier and acquired the ^{13}C NMR spectrum shown in Figure 5C. Two isotropic peaks separated by 2 ppm are observed, as reported by Huang et al., but these peaks are at higher frequencies. The high-frequency peak of this spectrum corresponds to the position of a single peak observed for a sample prepared in our laboratory (Figure 5 A and B). This experiment has been repeated several times; a value of $\delta_{\text{iso}} = 76$ ppm is consistently observed. A value of 76 ppm has also been reported by Oldfield and co-workers,²⁵ but it is not clear if their value is for a single peak or the average of two peaks. The commercial sample was dehydrated and the spectrum shown in Figure 5 D was obtained. A single peak is observed at the same frequency as for our samples. The two peaks observed for the commercial sample before dehydration may arise from separate peaks for the hydrate and anhydrous forms present in the sample or from two peaks for nonequivalent carbon atoms of a sample that is predominantly the hydrate form. In summary, the anhydrous form of Zeise's salt yields a single peak; our value for δ_{iso} , measured several times, is at higher frequency than those reported by Huang et al.²⁴

Figure 6 illustrates the ^{13}C NMR spectrum of a natural-abundance carbon sample of Zeise's salt. Although it was not possible to obtain a high-quality spectrum, the magnitudes of the CS tensor components can be estimated from this spectrum. The spectrum also places an upper limit on the span of the carbon CS tensor, $\Omega < 160$ ppm. Parameters derived from the fit of this spectrum were used as initial parameters in the fit of the spectra of the $^{13}\text{C}_2$ -labeled samples (vide infra). The calculated spectrum shown here is that which gave the best fit for all NMR spectra of this sample.

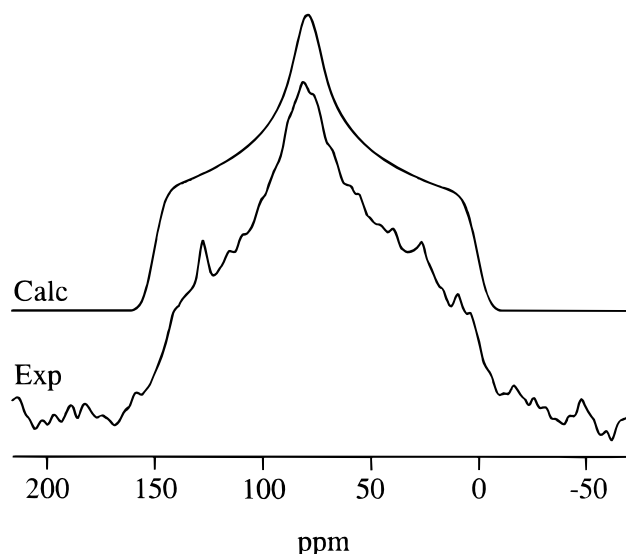


Figure 6. Calculated and simulated ^{13}C NMR spectra of a stationary natural-abundance carbon sample of Zeise's salt, acquired at 9.4 T; 642 transients were added.

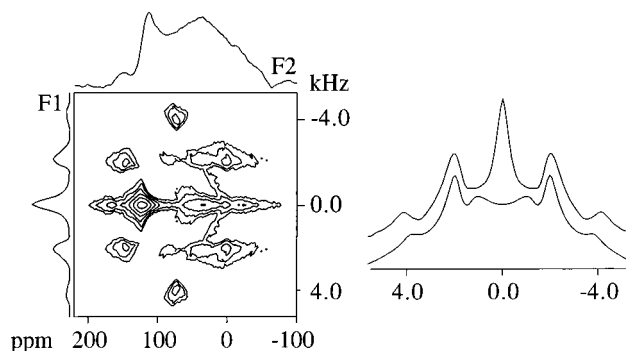


Figure 7. Two-dimensional ^{13}C spin-echo NMR spectrum of Zeise's salt acquired at 9.4 T; 32 transients were added for each of 64 t_1 increments. At right, the experimental (top) and calculated (bottom) F_1 projections are shown. The central peak is an experimental artifact.

The two-dimensional spin-echo NMR spectrum of Zeise's salt- $^{13}\text{C}_2$ is shown in Figure 7. Although the center of the F_1 projection is dominated by an experimental artifact, the "horns" arising from $R(^{13}\text{C},^{13}\text{C})$ are well resolved. The position of these peaks are very sensitive to the magnitude of $R(^{13}\text{C},^{13}\text{C})$, but insensitive to CS tensor parameters, allowing an accurate determination of this value. The fit of the F_1 projection, shown at the right of Figure 7, was achieved with $R(^{13}\text{C},^{13}\text{C}) = 2575 \pm 100$ Hz; the uncertainty here is based on the spectral resolution (approximately 190 Hz/point without zero filling). The value of $R(^{13}\text{C},^{13}\text{C})$ is less than the value predicted from the C,C bond length of 1.37 ± 0.03 Å,¹² 2950 ± 200 Hz (eq 2). Factors that might contribute to the reduced experimental value include vibrational motion of the C,C bond,⁵⁹ small amplitude torsional oscillations of the C,C bond (vide infra),^{5c} and the neglect of the contribution of $\Delta^1J(^{13}\text{C},^{13}\text{C})$ to R_{eff} .^{5f}

The shoulders of the F_1 projection at ± 4.0 kHz are not as well reproduced. Before considering this, it is useful to review the information available from the ^{13}C NMR experiments discussed above and the insight provided by the symmetry of the molecule. The observation of a single isotropic peak in spectra of MAS samples indicates that the two ^{13}C nuclei are crystallographically equivalent and hence will have the same principal components—these are known from the spectrum of the natural-abundance sample (Figure 6). The two CS tensors

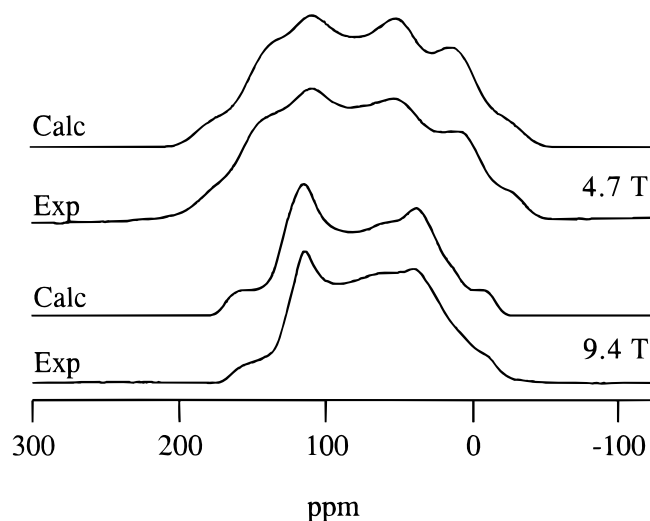


Figure 8. Calculated and experimental ^{13}C NMR spectra of a stationary sample of Zeise's salt- $^{13}\text{C}_2$, acquired at 4.7 and 9.4 T. 352 and 304 transients, respectively, were added for these spectra.

are related to each other by the same symmetry element as the carbon nuclei, C_2 . This fixes the angle α , which defines the relative orientation of the two CS tensors, to 0° . With a known $R(^{13}\text{C}, ^{13}\text{C})$, the only undetermined parameters are the Euler angles β and γ . The shoulders of the calculated $F1$ projection are very sensitive to γ and virtually insensitive to changes in the other CS tensor parameters. Since the one-dimensional spectra discussed below are also sensitive to this parameter, the parameters used to calculate the $F1$ projection are those that give a good fit to the latter, which have a much higher digital resolution. The discrepancy is thought to arise from the low digital resolution of the $F1$ projection. Further complications may arise from contributions to the experimental spectrum from the other magnetically active nuclei of the molecule ($^{35/37}\text{Cl}$, $I = 3/2$, natural abundance = 75.77 and 24.23%, respectively, and ^{195}Pt). We note that even in cases where all parameters are known from a single-crystal experiment, minor features of the $F1$ projection are not calculated exactly with this model.⁶⁰ In summary, the discrepancies between experimental and simulated spectra are thought to arise from experimental artifacts.

Carbon-13 NMR spectra of a stationary sample of Zeise's salt- $^{13}\text{C}_2$, with the corresponding calculated spectra, are shown in Figure 8; the CS tensor parameters derived from the simulation are summarized in Table 1. The spectra exhibit features characteristic of dipolar-coupled AB spin systems. Spectral features are broadened, a consequence of field-independent direct dipolar interactions with the magnetic nuclei of Zeise's salt. For example, based on $r_{\text{Pt,C}} = 2.14 \text{ \AA}$,¹² $R(^{13}\text{C}, ^{195}\text{Pt}) \approx 670 \text{ Hz}$. This is expected to produce some broadening to the base of the spectra. Likewise, values of $R(^{13}\text{C}, ^{35}\text{Cl})$ are approximately 35 and 100 Hz for coupling to the trans and cis chlorine atoms, respectively.¹² The effect is less evident in the spectrum acquired at 9.4 T because the anisotropy in the shielding is relatively larger (in frequency units). Line-broadening effects may also arise from intermolecular $^{13}\text{C}, ^{13}\text{C}$ dipolar interactions.

Calculated Carbon CS Tensors for Zeise's Salt. The calculated carbon CS tensors for Zeise's salt are summarized in Table 1. Agreement between experiment and theory is good. To investigate whether the different crystal forms of Zeise's salt are a factor in the observed shielding, calculations were performed with the structures of the anion of the hydrate¹⁴ and anhydrous¹² forms. Although two isotropic peaks are predicted

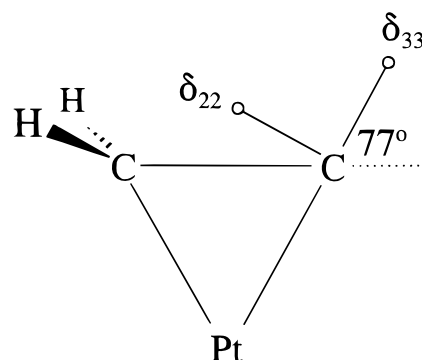


Figure 9. Orientation of the carbon CS tensor of Zeise's salt. The δ_{11} component is perpendicular to the page. The CS tensor about the other carbon atom is related to the one shown here by a C_2 rotation about an axis in the plane of the page bisecting the C,C bond. For clarity, the hydrogen atoms of the nucleus of interest and the chlorine atoms are omitted.

for both forms, that of the anhydrous form is predicted to be smaller and would be barely detectable experimentally. The calculated θ_{ii} values are also in good agreement with experiment (Table 1). Hence, an orientation for the carbon CS tensors is proposed, based on the combined experimental–theoretical results, as shown in Figure 9.

The magnitudes of the principal components (Table 1) are comparable to those reported by Oldfield et al., as are the orientations of the CS tensor components, which the authors calculated using density functional theory (DFT).²⁵ Ding and McDowell have reported the anisotropy, asymmetry, and orientation of the carbon CS tensors for Zeise's salt.²⁷ However, experimental errors are not indicated. Furthermore, they do not indicate how these parameters are defined and do not provide sufficient information to allow a comparison with our experimental results. Given that the $^{35/37}\text{Cl}, ^{13}\text{C}$ dipolar interaction is less than 100 Hz, the reliability of orientational information obtained from this interaction is unclear. We see no indication of any orientation-dependent broadening due to $^{35/37}\text{Cl}$ in our ^{13}C NMR spectra of stationary samples.

Comparison of the Carbon Chemical Shift Tensors for $\text{Pt}(\text{C}_2\text{H}_4)(\text{PPh}_3)_2$ and Zeise's Salt. The effect on the principal components of the carbon CS tensor of coordinating ethylene with Pt(0) and Pt(II) is shown graphically in Figure 10. The magnitudes of δ_{11} and δ_{22} decrease significantly; most affected is δ_{11} for $\text{Pt}(\text{C}_2\text{H}_4)(\text{PPh}_3)_2$, which is shielded by 171 ppm compared to the corresponding value for ethylene. In contrast, the magnitudes of δ_{33} are relatively insensitive to coordination. The orientations of the three principal components for Zeise's salt (Figure 9) as well as that of δ_{33} for $\text{Pt}(\text{C}_2\text{H}_4)(\text{PPh}_3)_2$ (Figure 4B) are comparable to those for uncoordinated ethylene (Figure 4A); the orientations of δ_{11} and δ_{22} for $\text{Pt}(\text{C}_2\text{H}_4)(\text{PPh}_3)_2$ (Figure 4C) are significantly different from those of ethylene.

The effect of coordination on the carbon CS tensors may be understood in terms of Ramsey's theory,⁶¹ in which nuclear magnetic shielding is partitioned into diamagnetic, σ^d , and paramagnetic, σ^p , terms. The diamagnetic term is positive, leading to greater shielding, whereas σ^p is usually negative, leading to deshielding. In general, σ^d shows a fairly weak orientation dependence. For example, the diamagnetic shielding perpendicular to the molecular plane of ethylene is estimated to be 337 ppm while the component in the molecular plane, perpendicular to the C,C bond, is 331 ppm and the component parallel to the C,C bond is 280 ppm.⁶² The corresponding values for σ^p are -78 , -382 , and -217 ppm .⁶² The large anisotropy in σ^p is a consequence of the electronic structure of ethylene.

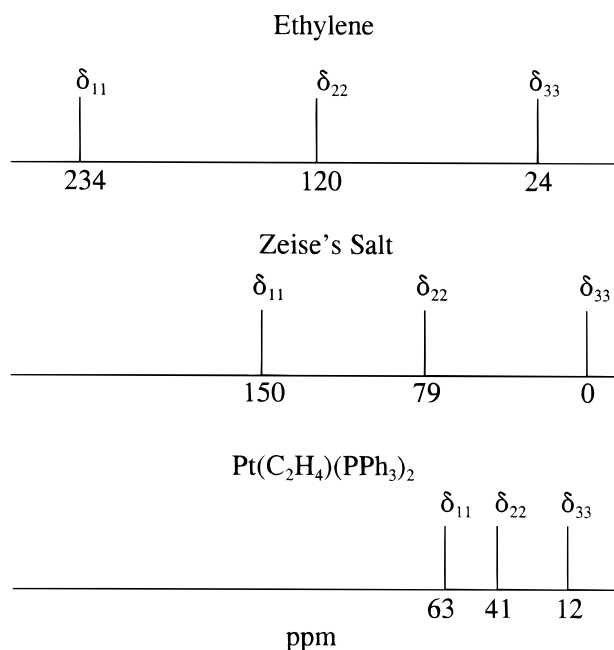


Figure 10. Comparison of the principal components of the carbon CS tensors for ethylene²³ with those of Zeise's salt and $\text{Pt}(\text{C}_2\text{H}_4)(\text{PPh}_3)_2$. Average values for the nonequivalent sites of the latter are illustrated.

Paramagnetic shielding involves the mixing of ground- and excited-state wave functions connected by magnetic-dipole allowed transitions such that charge appears to rotate about the direction of the applied magnetic field. Mixing of occupied and unoccupied molecular orbitals (MOs) about an axis perpendicular to the molecular plane of ethylene is either magnetic-dipole forbidden or there is a large difference in the energies of the MOs. Hence, δ_{33} lies in this general direction (Figure 4A). However, mixing of π and σ^* orbitals, resulting from "rotation" of orbitals about the axis in the molecular plane perpendicular to the C,C bond, contributes to the deshielding observed in this direction. Similarly, mixing of the σ and π^* orbitals, resulting from "rotation" about the C,C bond, contributes to the deshielding observed in the direction parallel to the bond. In summary, δ_{33} is relatively insensitive to coordination with platinum because the dominant term in the total shielding in this direction is σ^d which is less sensitive than σ^p , a much more important component of the total shielding in the directions of δ_{11} and δ_{22} .

An ethylene ligand coordinated to a metal center is expected to have properties intermediate between those of ethylene and ethane.² The observed sensitivity of δ_{11} and δ_{22} and the insensitivity of δ_{33} to coordination is consistent with this hypothesis. Molecular orbitals with magnetic-dipole allowed symmetry in ethane are separated by a relatively large energy difference, precluding efficient mixing and resulting in a small σ^p term for all three tensor components.⁶¹ Hence, the magnitudes of the principal components of the carbon CS tensors of ethane, $\delta_{11} = \delta_{22} = 11$ ppm and $\delta_{33} = 4$ ppm,⁶³ are comparable to δ_{33} for ethylene. The mixing of π and σ MOs in the platinum-ethylene complexes is allowed, but to a smaller extent than for uncoordinated ethylene, leading to a smaller paramagnetic term and thus to increased shielding in the directions corresponding to δ_{11} and δ_{22} . Hence, as expected, the δ_{11} and δ_{22} components are intermediate between those of ethane and ethylene, and δ_{33} is similar for all compounds (Table 1). The greater sensitivity of the CS tensor for $\text{Pt}(\text{C}_2\text{H}_4)(\text{PPh}_3)_2$ to coordination is also consistent with this model, since the structure of the ethylene ligand is significantly modified in this strong coordination

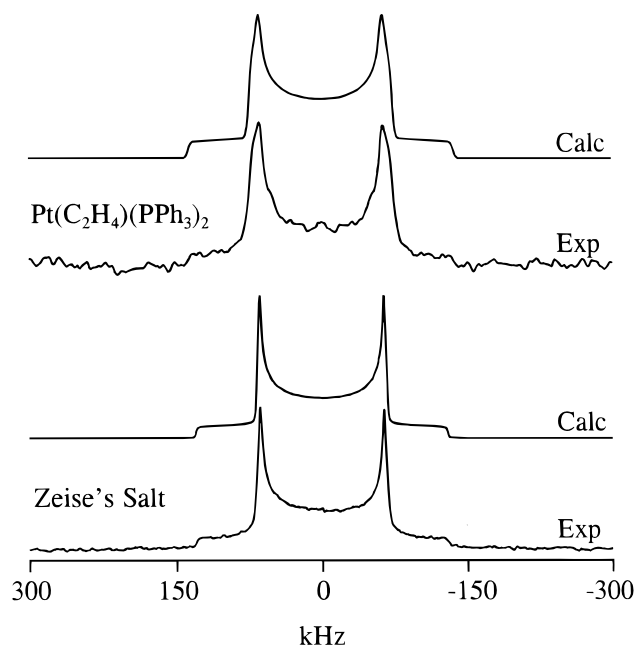


Figure 11. Calculated and experimental ^2H NMR spectra of stationary samples of $\text{Pt}(\text{C}_2\text{H}_4)(\text{PPh}_3)_2$ and Zeise's salt- $^2\text{H}_4$. Both spectra were acquired at 9.4 T, with 80 and 49 transients, respectively, for $\text{Pt}(\text{C}_2\text{H}_4)(\text{PPh}_3)_2$ and Zeise's salt.

complex. We note that although the structure of the ethylene ligand is only slightly modified in Zeise's salt,¹² the carbon CS tensor is significantly different from that of ethylene. This illustrates the high sensitivity of nuclear magnetic shielding to symmetry and to subtle variations in chemical bonding.

The isotropic carbon chemical shifts of ethylene and Zeise's salt calculated by first principles reproduce the experimental values; however, examination of the individual tensor components indicates that this is partly due to cancellation of errors. More accurate results would be expected if the effects of electron correlation were included, but such calculations are not practical at this time on the large molecules considered here. The ab initio calculations also accurately predict the effect of coordination to platinum on the CS tensor components, including the greater effect of coordination to $\text{Pt}(0)$.

In light of the ensuing discussion on the dynamics of the ethylene ligand in these complexes, it may be assumed that the carbon CS tensors of these compounds are not subject to motional averaging.

Internal Dynamics of the Platinum-Ethylene Complexes. NMR. The calculated and experimental ^2H NMR spectra of stationary samples of $\text{Pt}(\text{C}_2\text{H}_4)(\text{PPh}_3)_2$ and Zeise's salt- $^2\text{H}_4$ are shown in Figure 11. The ^2H magnetization is slow to relax (vide infra), particularly for $\text{Pt}(\text{C}_2\text{H}_4)(\text{PPh}_3)_2$ which requires a 1.5 h recycle delay. The spectrum of this compound (upper trace) has a poor signal-to-noise ratio, but the ^2H quadrupolar parameters may be determined from the "horns" of the Pake doublet. The ^2H relaxation time of Zeise's salt also is long, requiring 20 min recycle delays, but a well-resolved spectrum (Figure 11, lower trace) was acquired. The ^2H quadrupolar parameters derived from the simulations are $C_Q = 181 \pm 4$ kHz and $\eta = 0.075 \pm 0.020$ for $\text{Pt}(\text{C}_2\text{H}_4)(\text{PPh}_3)_2$, and $C_Q = 173 \pm 2$ kHz and $\eta = 0.025 \pm 0.020$ for Zeise's salt. These parameters are comparable to those reported for ethylene- $^2\text{H}_1$: $C_Q = 175.3 \pm 1.3$ kHz and $\eta = 0.039 \pm 0.001$,⁶⁴ and for ethane- $^2\text{H}_6$: $C_Q = 168 \pm 3$ kHz and $\eta = 0.0$.⁶⁵ The reported ^2H quadrupolar parameters for ethylene⁶⁴ and ethane⁶⁵ are those expected in the absence of motional averaging. An ab initio calculation of the ^2H EFG

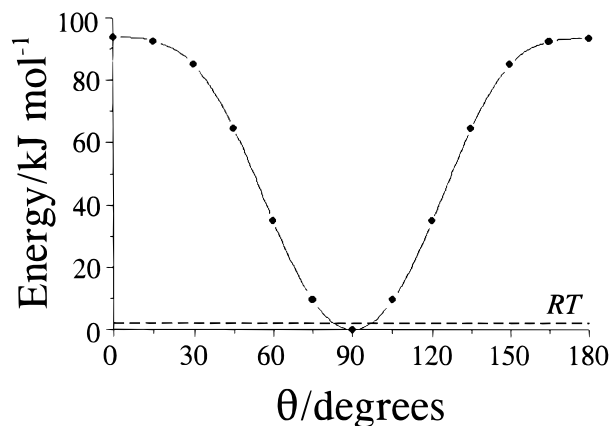


Figure 12. Calculated barrier to internal rotation of the ethylene ligand in Zeise's salt. The angle θ defines the angle formed by the C,C bond with the PtCl_3 plane. The dashed line corresponds to RT at 300 K; the solid curve is a fit to the calculated points.

tensors at the HF/cc-pVQZ level predicts virtually identical quadrupolar parameters for ethylene and Zeise's salt.

The ^2H NMR parameters for the platinum–ethylene complexes are comparable to those expected for the ligand in the absence of motion, allowing us to assert that the ethylene ligands in these complexes are not undergoing large-amplitude motion. The observed ^2H NMR spectra (Figure 11) do not preclude small-amplitude motions of the ethylene ligand;⁶⁶ the long ^2H T_1 s suggest that any such motions must be ineffective in causing relaxation.⁶⁷ A determination of T_1 via the inversion recovery experiment⁶⁸ would be instructive but is impractical because of the long recycle delays required.

Using a model proposed by Zilm and Grant,^{5c} the observed value of $R(^{13}\text{C},^{13}\text{C})$ for Zeise's salt (vide supra) compared to that expected from the C,C bond length¹² (eq 2), implies that torsional motion of the C,C bond can be about a cone angle as large as 20° , depending on the magnitude of the vibrational correction. For $\text{Pt}(\text{C}_2\text{H}_4)(\text{PPh}_3)_2$, the measured value of $R(^{13}\text{C},^{13}\text{C})$ is close to that expected from the experimental C,C bond length,⁹ consistent with the conclusion that the ethylene ligand is rigid in this complex.

A Computational Study of the Internal Dynamics. Figure 12 illustrates the calculated barrier to internal rotation of the ethylene ligand in Zeise's salt. The large barrier, 93 kJ mol^{-1} , suggests that the ethylene ligand does not rotate, in agreement with our experimental results. If one assumes a Boltzmann distribution of orientations of the ethylene ligand, there is a low probability that the ethylene will deviate from its most stable conformation by more than an energy difference of RT , where R is the gas constant and T is the temperature. The dashed line in Figure 12 illustrates this value for 300 K; the ethylene may be expected to fluctuate about the minimum, but not to orientations that place the energy of the compound significantly above the dashed line. Clearly, large-amplitude motion is not expected, although motion of $\pm 10^\circ$ is allowed with this model. These results must be considered in light of the necessary approximations of this model. In particular, these calculations are for an isolated molecule and hence do not consider intermolecular effects, which might further restrict the motion of the ethylene. Single-point HF calculations on $\text{Pt}(\text{C}_2\text{H}_4)(\text{PPh}_3)_2$, with the ethylene oriented in and perpendicular to the plane defined by the platinum and the two phosphorus atoms, correctly predict that the planar conformation of the ethylene is favored, with an 85 kJ mol^{-1} difference between the two conformers. These results are comparable to those of an early

computational study on isolated molecules using the extended Hückel method, which predicts barriers to internal rotation of approximately 80 kJ mol^{-1} for the ethylene ligand in Zeise's salt, a value only slightly lower than that calculated for $\text{Pt}(\text{C}_2\text{H}_4)(\text{PPh}_3)_2$.⁶⁹ A recent study of $\text{Pt}(\text{C}_2\text{H}_4)(\text{PPh}_3)_2$ using DFT predicts a large barrier to internal motion of the ethylene ligand, 149 kJ mol^{-1} ; the favored conformation places the ethylene in the plane defined by the platinum and phosphorus atoms.⁷⁰ Calculations by Ziegler and co-workers have shown that relativistic effects are an important factor in the Pt–ethylene bonding of this complex.⁷¹

Our investigation of the internal dynamics of the ethylene ligand of $\text{Pt}(\text{C}_2\text{H}_4)(\text{PPh}_3)_2$ confirms previous observations that this ligand is not subject to significant motion at 300 K. The ^2H NMR study of Zeise's salt demonstrates that the ethylene ligand in this complex does not undergo large-amplitude motion, a conclusion that is supported by ab initio calculations.

Conclusions

The carbon chemical shift tensors for $\text{Pt}(\text{C}_2\text{H}_4)(\text{PPh}_3)_2$ and Zeise's salt, $\text{K}[\text{Pt}(\text{C}_2\text{H}_4)\text{Cl}_3]$, have been characterized by solid-state NMR. The magnitudes of the δ_{11} and δ_{22} components of the carbon CS tensors for ethylene are very sensitive to coordination with platinum, decreasing significantly, but the δ_{33} components are virtually unaffected. The CS tensors are particularly sensitive to coordination of ethylene with Pt(0), but coordination with Pt(II) also leads to significant changes in the CS tensors. These effects have been rationalized in terms of Ramsey's theory of nuclear magnetic shielding and the structural modifications that occur upon coordination with Pt(0) and Pt(II). Agreement between theoretical and experimental carbon chemical shift tensors is generally good. Hence, orientations for the CS tensors in the molecular framework have been proposed on the basis of the experimental–theoretical results. The large differences between the olefinic carbon CS tensors of ethylene and $\text{Pt}(\text{C}_2\text{H}_4)(\text{PPh}_3)_2$ are comparable to those found between the CS tensors of *trans*-stilbene and $\text{Pt}(\eta^2\text{-trans-stilbene})(\text{PPh}_3)_2$.²¹

A ^2H NMR study of the ethylene- $^2\text{H}_4$ derivatives of these molecules shows that the ethylene ligands in these compounds are not subject to significant motion in the solid state at 300 K. This conclusion is supported by ab initio calculations of the barrier to internal rotation of the ethylene ligand. Hence, the carbon chemical shift tensors reported herein are those expected in the absence of motional averaging.

Acknowledgment. The Natural Sciences and Engineering Research Council of Canada (NSERC) is acknowledged for a research grant. We are grateful to Dr. Beata Kolakowski for obtaining mass spectra, to Mr. Chris McDonald for his assistance in the preparation of $\text{Pt}(\text{C}_2\text{H}_4)(\text{PPh}_3)_2$, to Dr. Roland Rösler for his help in the preparation of Zeise's salt, and to Drs. Klaus Eichele and Gang Wu for some preliminary work on this project. We thank Mr. David Bryce, Ms. Shelley Forgeron, Ms. Myrlene Gee, and Dr. Mike Lumsden for their help and encouragement. G.M.B. thanks NSERC, the Walter C. Sumner Foundation, and the Izaak Walton Killam Trust for postgraduate scholarships. All spectra were acquired at the Atlantic Region Magnetic Resonance Centre, also funded by NSERC.

References and Notes

- (1) (a) Zeise, W. C. *Pogg. Ann. Phys.* **1827**, 9, 632. (b) Zeise, W. C. *Pogg. Ann. Phys.* **1831**, 21, 497. (c) For an English-language translation of reference (b), see Kauffman, G. B. *Classics in Coordination Chemistry*,

Part II: Selected Papers; Dover: New York, 1976; p 17. References (a) and (b) are cited from this text.

- (2) (a) Hartley, F. R. In *Comprehensive Organometallic Chemistry*; Wilkinson, G., Ed.; Pergamon: Oxford, 1982; Vol. 6, p 471. (b) Young, G. B. In *Comprehensive Organometallic Chemistry II*; Abel, E. W., Stone, F. G. A., Wilkinson, G., Puddephatt, R. J., Eds.; Pergamon: New York, 1995; Vol. 9, p 533. (c) Huheey, J. E.; Keiter, E. A.; Keiter, R. L. *Inorganic Chemistry*, 4th ed.; HarperCollins College: New York, 1993; p 662.
- (3) For continuity, the terms "olefinic" or "ethylenic" will be used to describe the olefinic atoms of the uncoordinated ligand or the corresponding atoms of the complex, although in the latter case this does not correspond to a strict definition of the terms.
- (4) Eichele, K.; Wasylishen, R. E. *J. Magn. Reson.* **1994**, *106A*, 46.
- (5) (a) Power, W. P.; Wasylishen, R. E. *Ann. Rep. NMR Spectrosc.* **1991**, *23*, 1. (b) van Willigen, H.; Griffin, R. G.; Haberkorn, R. A. *J. Chem. Phys.* **1977**, *67*, 5855. (c) Zilm, K. W.; Grant, D. M. *J. Am. Chem. Soc.* **1981**, *103*, 2913. (d) Curtis, R. D.; Hilborn, J. W.; Wu, G.; Lumsden, M. D.; Wasylishen, R. E.; Pincock, J. A. *J. Phys. Chem.* **1993**, *97*, 1856. (e) Lumsden, M. D.; Wu, G.; Wasylishen, R. E.; Curtis, R. D. *J. Am. Chem. Soc.* **1993**, *115*, 2825. (f) Wasylishen, R. E. In *Encyclopedia of Nuclear Magnetic Resonance*; Grant, D. M., Harris, R. K., Eds.; John Wiley and Sons: Chichester, 1996; p 1685.
- (6) (a) Facelli, J. C. In *Encyclopedia of Nuclear Magnetic Resonance*; Grant, D. M.; Harris, R. K., Eds.; John Wiley and Sons: Chichester, 1996; p 4327. (b) Jameson, C. J.; de Dios, A. C. In *Nuclear Magnetic Resonance—A Specialist Periodical Report*; Webb, G. A., Ed.; Royal Society of Chemistry: Cambridge, U.K., 1999; Vol. 28, Chapter 2, and previous volumes of this annual series. (c) Bernard, G. M.; Wu, G.; Lumsden, M. D.; Wasylishen, R. E.; Maigrot, N.; Charrier, C.; Mathey, F. *J. Phys. Chem. A* **1999**, *103*, 1029. (d) de Dios, A. C.; Roach, J. L.; Walling, A. E. In *Modeling NMR Chemical Shifts*; Facelli, J. C.; de Dios, A. C., Eds.; American Chemical Society: Washington, DC, 1999; Chapter 16.
- (7) (a) Ditchfield, R. *Mol. Phys.* **1974**, *27*, 789. (b) Wolinski, K.; Hinton, J. F.; Pulay, P. *J. Am. Chem. Soc.* **1990**, *112*, 8251. (c) Rauhut, G.; Puyear, S.; Wolinski, K.; Pulay, P. *J. Phys. Chem.* **1996**, *100*, 6310.
- (8) (a) Griffin, R. G.; Beshah, K.; Ebelhäuser, R.; Huang, T. H.; Olejniczak, E. T.; Rice, D. M.; Siminovich, D. J.; Wittebort, R. J. In *The Time Domain in Surface and Structural Dynamics*; Long, G. J., Grandjean, F., Eds.; Kluwer Academic: Dordrecht, 1988; Chapter 7. (b) Davis, J. H. In *Isotopes in the Physical and Biomedical Sciences*; Buncel, E., Jones, J. R., Eds.; Elsevier: Amsterdam, 1991; Vol. 2, Chapter 3. (c) Hoatson, G. L.; Vold, R. L. *NMR Basic Princ. Prog.* **1994**, *32*, 1. (d) Tycko, R. In *Understanding Chemical Reactivity*; Mezey, P. G., Ed.; Kluwer Academic: Dordrecht, 1994; Vol. 8. (e) Batchelder, L. S. In *Encyclopedia of Nuclear Magnetic Resonance*; Grant, D. M., Harris, R. K., Eds.; John Wiley and Sons: Chichester, 1996; p 1574. (f) Chandrakumar, N. *NMR Basic Princ. Prog.* **1996**, *34*, 1.
- (9) Cheng, P.-T.; Nyburg, S. C. *Can. J. Chem.* **1972**, *50*, 912.
- (10) Duncan, J. L. *Mol. Phys.* **1974**, *28*, 1177.
- (11) Hirota, E.; Endo, Y.; Saito, S.; Duncan, J. L. *J. Mol. Spectrosc.* **1981**, *89*, 285.
- (12) Eller, P. G.; Ryan, R. R.; Schaeffer, R. O. *Cryst. Struct. Commun.* **1977**, *6*, 163.
- (13) Jarvis, J. A. J.; Kilbourn, B. T.; Owston, P. G. *Acta Crystallogr.* **1971**, *B27*, 366.
- (14) Love, R. A.; Koetzle, T. F.; Williams, G. J. B.; Andrews, L. C.; Bau, R. *Inorg. Chem.* **1975**, *14*, 2653.
- (15) (a) Dewar, M. J. S. *Bull. Soc. Chim. Fr.* **1951**, *18*, C71. (b) Chatt, J.; Duncanson, L. A. *J. Chem. Soc.* **1953**, 2939.
- (16) Mann, B. E.; Taylor, B. F. *¹³C NMR Data for Organometallic Compounds*; Academic: London, 1981.
- (17) (a) Chisholm, M. H.; Clark, H. C.; Manzer, L. E.; Stothers, J. B. *J. Am. Chem. Soc.* **1972**, *94*, 5087. (b) Chaloner, P. A.; Davies, S. E.; Hitchcock, P. B. *Polyhedron* **1997**, *16*, 765.
- (18) For a compilation of carbon chemical shift tensors see Duncan, T. M. *A Compilation of Chemical Shift Anisotropies*; Farragut: Chicago, 1990; p C-1.
- (19) Wallraff, G. M. Ph.D. Thesis, University of Utah, 1985.
- (20) Gay, I. D.; Young, G. B. *Organometallics* **1996**, *15*, 2264.
- (21) Bernard, G. M.; Wu, G.; Wasylishen, R. E. *J. Phys. Chem. A* **1998**, *102*, 3184.
- (22) (a) Farnell, L. F.; Randall, E. W.; Rosenberg, E. *Chem. Commun.* **1971**, 1078. (b) Cooper, D. G.; Powell, J. *Inorg. Chem.* **1976**, *15*, 1959. (c) Meester, M. A. M.; Stufkens, D. J.; Vrieze, K. *Inorg. Chim. Acta* **1976**, *16*, 191. (d) Meester, M. A. M.; Stufkens, D. J.; Vrieze, K. *Inorg. Chim. Acta* **1977**, *21*, 251.
- (23) Zilm, K. W.; Conlin, R. T.; Grant, D. M.; Michl, J. *J. Am. Chem. Soc.* **1980**, *102*, 6672.
- (24) Huang, Y.; Gilson, D. F. R.; Butler, I. S. *J. Chem. Soc., Dalton Trans.* **1992**, 2881.
- (25) Havlin, R.; McMahon, M.; Srinivasan, R.; Le, H.; Oldfield, E. J. *Phys. Chem. A* **1997**, *101*, 8908.
- (26) Herzfeld, J.; Berger, A. E. *J. Chem. Phys.* **1980**, *73*, 6021.

- (27) Ding, S.; McDowell, C. A. *Chem. Phys. Lett.* **1997**, *268*, 194.
- (28) Challoner, R.; Sebald, A. *Solid State Nucl. Magn. Reson.* **1995**, *4*, 39.
- (29) Mann, B. E. In *Comprehensive Organometallic Chemistry*; Wilkinson, G., Ed.; Pergamon: Oxford, 1982; Vol. 3, p 89.
- (30) Vierkötter, S. A.; Barnes, C. E. *J. Am. Chem. Soc.* **1994**, *116*, 7445.
- (31) Gallop, M. A.; Johnson, B. F. G.; Keeler, J.; Lewis, J.; Heyes, S. J.; Dobson, C. M. *J. Am. Chem. Soc.* **1992**, *114*, 2510.
- (32) Slichter, C. P. *Principles of Magnetic Resonance*, 3rd ed.; Springer-Verlag: Berlin, 1990; Chapter 3.
- (33) Reeves, L. W. *Can. J. Chem.* **1960**, *38*, 736.
- (34) Maričić, S.; Redpath, C. R.; Smith, J. A. S. *J. Chem. Soc.* **1963**, 4905.
- (35) Blake, D. M.; Roundhill, D. M. *Inorg. Synth.* **1978**, *18*, 120.
- (36) Chock, P. B.; Halpern, J.; Paulik, F. E. *Inorg. Synth.* **1990**, *28*, 349.
- (37) (a) Pines, A.; Gibby, M. G.; Waugh, J. S. *J. Chem. Phys.* **1972**, *56*, 1776. (b) Pines, A.; Gibby, M. G.; Waugh, J. S. *J. Chem. Phys.* **1973**, *59*, 569.
- (38) Earl, W. L.; VanderHart, D. L. *J. Magn. Reson.* **1982**, *48*, 35.
- (39) Alderman, D. W.; Solum, M. S.; Grant, D. M. *J. Chem. Phys.* **1986**, *84*, 3717.
- (40) Mason, J. *Solid State Nucl. Magn. Reson.* **1993**, *2*, 285.
- (41) (a) Eichele, K.; Wu, G.; Wasylishen, R. E.; Britten, J. F. *J. Phys. Chem.* **1995**, *99*, 1030. (b) Rance, M.; Byrd, R. A. *J. Magn. Reson.* **1983**, *52*, 221.
- (42) (a) Haerberlen, U. In *Advances in Magnetic Resonance*, Supplement 1; Waugh, J. S., Ed.; Academic Press: New York, 1976. (b) Schmidt-Rohr, K.; Spiess, H. W. *Multidimensional Solid-State NMR and Polymers*; Academic Press: London, 1994.
- (43) (a) Zilm, K. W.; Webb, G. G.; Cowley, A. H.; Pakulski, M.; Orendt, A. *J. Am. Chem. Soc.* **1988**, *110*, 2032. (b) Nakai, T.; McDowell, C. A. *J. Am. Chem. Soc.* **1994**, *116*, 6373. (c) Nakai, T.; McDowell, C. A. *Solid State Nucl. Magn. Reson.* **1995**, *4*, 163. (d) Eichele, K.; Wasylishen, R. E.; Schurko, R. W.; Burford, N.; Whitla, W. A. *Can. J. Chem.* **1996**, *74*, 2372. (e) Gee, M.; Wasylishen, R. E.; Eichele, K.; Wu, G.; Cameron, T. S.; Mathey, F.; Laporte, F. *Can. J. Chem.* **2000**, *78*, 118.
- (44) Davis, J. H.; Jeffrey, K. R.; Bloom, M.; Valic, M. I.; Higgs, T. P. *Chem. Phys. Lett.* **1976**, *42*, 390.
- (45) Henrichs, P. M.; Hewitt, J. M.; Linder, M. *J. Magn. Reson.* **1984**, *60*, 280.
- (46) Frisch, M. J.; Trucks, G. W.; Schlegel, H. B.; Scuseria, G. E.; Robb, M. A.; Cheeseman, J. R.; Zakrzewski, V. G.; Montgomery, J. A., Jr.; Stratmann, R. E.; Burant, J. C.; Dapprich, S.; Millam, J. M.; Daniels, A. D.; Kudin, K. N.; Strain, M. C.; Farkas, O.; Tomasi, J.; Barone, V.; Cossi, M.; Cammi, R.; Mennucci, B.; Pomelli, C.; Adamo, C.; Clifford, S.; Ochterski, J.; Petersson, G. A.; Ayala, P. Y.; Cui, Q.; Morokuma, K.; Malick, D. K.; Rabuck, A. D.; Raghavachari, K.; Foresman, J. B.; Cioslowski, J.; Ortiz, J. V.; Stefanov, B. B.; Liu, G.; Liashenko, A.; Piskorz, P.; Komaromi, I.; Gomperts, R.; Martin, R. L.; Fox, D. J.; Keith, T.; Al-Laham, M. A.; Peng, C. Y.; Nanayakkara, A.; Gonzalez, C.; Challacombe, M.; Gill, P. M. W.; Johnson, B.; Chen, W.; Wong, M. W.; Andres, J. L.; Gonzalez, C.; Head-Gordon, M.; Replogle, E. S.; Pople, J. A. *Gaussian 98*, Revision A.4; Gaussian, Inc.: Pittsburgh, PA, 1998.
- (47) (a) Chesnut, D. B.; Moore, K. D. *J. Comput. Chem.* **1989**, *10*, 648. (b) Chesnut, D. B.; Rusiloski, B. E.; Moore, K. D.; Egoal, D. A. *J. Comput. Chem.* **1993**, *14*, 1364.
- (48) (a) Hay, P. J.; Wadt, W. R. *J. Chem. Phys.* **1985**, *82*, 270. (b) Wadt, W. R.; Hay, P. J. *J. Chem. Phys.* **1985**, *82*, 284. (c) Hay, P. J.; Wadt, W. R. *J. Chem. Phys.* **1985**, *82*, 299.
- (49) Jameson, A. K.; Jameson, C. J. *Chem. Phys. Lett.* **1987**, *134*, 461.
- (50) Frisch, M. J.; Head-Gordon, M.; Pople, J. A. *Chem. Phys. Lett.* **1990**, *166*, 281.
- (51) (a) Hall, P. W.; Puddephatt, R. J.; Tipper, C. F. H. *J. Organomet. Chem.* **1974**, *71*, 145. (b) Wrackmeyer, B. *Z. Naturforsch.* **1997**, *52b*, 1019.
- (52) (a) Wu, G.; Wasylishen, R. E. *J. Magn. Reson.* **1993**, *102A*, 183. (b) Wu, G.; Wasylishen, R. E. *J. Chem. Phys.* **1993**, *99*, 6321. (c) Wu, G.; Sun, B.; Wasylishen, R. E.; Griffin, R. G. *J. Magn. Reson.* **1997**, *124*, 366. (d) Dusold, S.; Klaus, E.; Sebald, A.; Bak, M.; Nielsen, N. C. *J. Am. Chem. Soc.* **1997**, *119*, 7121.
- (53) Diehl, P.; Sýkora, S.; Wullschleger, E. *Mol. Phys.* **1975**, *29*, 305.
- (54) Kaski, J.; Lantto, P.; Vaara, J.; Jokisaari, J. *J. Am. Chem. Soc.* **1998**, *120*, 3993.
- (55) Lumsden, M. D.; Wasylishen, R. E.; Britten, J. F. *J. Phys. Chem.* **1995**, *99*, 16602.
- (56) Eichele, K.; Ossenkamp, G. C.; Wasylishen, R. E.; Cameron, T. S. *Inorg. Chem.* **1999**, *38*, 639.
- (57) (a) Spiess, H. W. *NMR Basic Princ. Prog.* **1978**, *15*, 55. (b) Wolff, E. K.; Griffin, R. G.; Waugh, J. S. *J. Chem. Phys.* **1977**, *67*, 2387. (c) Mehring, M. *Principles of High-Resolution NMR in Solids*; Springer-Verlag: Berlin, 1983; Chapter 7. (d) Veeman, W. S. *Prog. NMR Spectrosc.* **1984**, *16*, 193.

- (58) (a) Alarcón, S. H.; Olivieri, A. C.; Harris, R. K. *Solid State Nucl. Magn. Reson.* **1993**, *2*, 325. (b) Eichele, K.; Wasylishen, R. E.; Grossert, J. S.; Olivieri, A. *J. Phys. Chem.* **1995**, *99*, 10110.
- (59) Ishii, Y.; Terao, T.; Hayashi, S. *J. Chem. Phys.* **1997**, *107*, 2760.
- (60) Gee, M.; Wasylishen, R. E.; Eichele, K.; Britten, J. F. *J. Phys. Chem. A* **2000**, *104*, 4598.
- (61) (a) Ramsey, N. F. *Phys. Rev.* **1950**, *78*, 699. (b) For a general discussion of Ramsey's theory as it pertains to NMR parameters, see Jameson, C. J.; Mason, J. In *Multinuclear NMR*; Mason, J., Ed.; Plenum: New York, 1987; Chapter 3. (c) Schreckenbach, G.; Dickson, R. M.; Ruiz-Morales, Y.; Ziegler, T. In *Chemical Applications of Density-Functional Theory*; ACS Symposium Series 629; Laird, B. B.; Ross, R. B.; Ziegler, T., Eds.; American Chemical Society: Washington, DC, 1996; Chapter 23.
- (62) Zilm, K. W.; Duchamp, J. C. In *Nuclear Magnetic Shieldings and Molecular Structure*; Tossell, J. A., Ed.; Kluwer Academic: Dordrecht, 1993; p 315.
- (63) Solum, M. S.; Facelli, J. C.; Michl, J.; Grant, D. M. *J. Am. Chem. Soc.* **1986**, *108*, 6464.
- (64) Kowalewski, J.; Lindblom, T.; Vestin, R.; Drakenberg, T. *Mol. Phys.* **1976**, *31*, 1669.
- (65) Burnett, L. J.; Muller, B. H. *J. Chem. Phys.* **1971**, *55*, 5829.
- (66) Vold, R. R.; Vold, R. L. *Adv. Magn. Opt. Reson.* **1991**, *16*, 85.
- (67) Alla, M.; Eckman, R.; Pines, A. *Chem. Phys. Lett.* **1980**, *71*, 148.
- (68) Wasylishen, R. E. In *NMR Spectroscopy Techniques*, 2nd ed.; Bruch, M. D., Ed.; Marcel Dekker: New York, 1996; Chapter 3.
- (69) Albright, T. A.; Hoffman, R.; Thibeault, J. C.; Thorn, D. L. *J. Am. Chem. Soc.* **1979**, *101*, 3801.
- (70) Nunzi, F.; Sgamellotti, A.; Re, N.; Floriani, C. *J. Chem. Soc., Dalton Trans.* **1999**, 3487.
- (71) Li, J.; Schreckenbach, G.; Ziegler, T. *Inorg. Chem.* **1995**, *34*, 3245.